Review

Cluster-Based Coordination Polymers of Mn/Fe-Oxo Pivalates and Isobutyrates [†]

Svetlana Baca [1,*] and **Paul Kögerler** [2]

[1]   Institute of Applied Physics, Academiei 5, 2028 Chisinau, Moldova
[2]   Institute of Inorganic Chemistry, RWTH Aachen University, Landoltweg 1, 52074 Aachen, Germany; paul.koegerler@ac.rwth-aachen.de
[*]   Correspondence: sbaca_md@yahoo.com; Tel.: +373-2-273-9661
[†]   Dedicated to Professor Christoph Janiak on the occasion of his 60th birthday.

Abstract: Polynuclear coordination clusters can be readily arranged in cluster-based coordination polymers (CCPs) by appropriate bridging linkers. This review provides an overview of our recent developments in exploring structurally well-defined Mn/Fe-oxo pivalate and isobutyrate building blocks in the formation of CCPs assemblies with an emphasis on synthetic strategies and magnetic properties.

Keywords: cluster-based coordination polymer; carboxylate; iron(III); manganese(II,III)

1. Introduction

Cluster-based coordination polymers (CCPs) have received significant attention over the past decade due to their promising potential as multifunctional materials for technological and industrial applications [1–6]. Typically, CCPs are constructed from metal coordination clusters that are bridged by polytopic organic ligands forming multidimensional systems such as one-dimensional (1D) chains, two-dimensional (2D) layers and three-dimensional (3D) metal–organic frameworks (MOFs) [7]. Two synthetic pathways have been explored by synthetic chemists for the fabrication of the CCPs. In formation reactions, one can utilize simple salts or presynthesized well-defined polynuclear metal clusters, following Robson's classical node (typically consisting of a single metal ion) and spacer (polytopic coordination ligand) approach [8] or Yaghi and O'Keeffe's "secondary building units" (SBUs, representing a rigid metal carboxylate cluster with external connectivity that mimics triangle, square, tetrahedral, hexagonal or octahedral patterns) strategy [9,10]. Later, Zaworotko et al. developed a design strategy that exploits metal–organic polyhedra as "supermolecular building blocks" (SBBs), which combine a greater range of scale (nanometer scale) and high symmetry and, thus, can afford improved control over the topology of the resulting coordination polymers [11].

To date, considerable efforts have been devoted to developing a range of CCPs by using rigid carboxylate clusters of paramagnetic transition metals as building units that contain multiple metal ions linked by multiple coordination ligands, especially for producing molecular magnetic arrays [12]. In comparison to other typically employed structural building blocks, polynuclear carboxylate-based clusters offer distinct advantages for engineering CCPs: (i) they can afford specific control over a CCPs' topology through precise adjusting the coordination environment of metal ions and thus providing the easy accessibility of spacers to a vacant coordination site at the periphery of the cluster, to which a separate cluster can be attached; (ii) ease in managing and fine-tuning their shape and size via increasing or decreasing the nuclearity; (iii) and feasibility to vary their physical properties since their physical characteristics (magnetic, spectroscopic and redox behavior) can be determined and modified prior to network formation [4,5]. Furthermore, the carboxylate ligands can be partially substituted, e.g., by redox-active inorganic ligands such as

magnetically functionalized polyoxoanions [13] or paramagnetic organic ligands [14–17]; thus, the final assemblies can reveal some additional properties and functions such as charge-state switching of magnetic ground states and anisotropy. Such tailor-made multidimensional CCPs can be applied in numerous important fields such as catalysis, gas storage, pharmaceuticals, etc. [18].

Mn/Fe-oxo carboxylate clusters incorporating multiple spin centers exhibit fascinating magnetic phenomena such as single-molecule magnet behavior (SMM) [19–21] and represent useful building blocks for the creation of Mn and Fe-based CCPs. In particular, Christou, Tasiopoulos et al. [22] prepared 3D CCPs with nanometer-sized channels that exhibit SMM characteristics and are based on large polynuclear $\{Mn_{19}O_{10}\}$ acetate building units, $[Mn_{19}NaO_{10}(OH)_4(ac)_9(pd)_9(H_2O)_3]_n$ and $[Mn_{19}NaO_{10}(OH)_4(ac)_9(mpd)_9(H_2O)_3]_n$ (where Hac = acetic acid), using 1,3-propanediol (H_2pd) and 2-methyl-1,3-propanediol (H_2mpd). Later, fascinating extended networks based on polynuclear $\{Mn_{17}O_8\}$ acetate building units connected by N_3^- or OCN^- anions into 1D and 2D CCPs, namely $[Mn_{17}O_8(ac)_4(pd)_{10}(py)_6(N_3)_5]_n$, $[Mn_{17}O_8(ac)_4(mpd)_{10}(py)_8(N_3)_5]_n$ and $[Mn_{17}O_8(ac)_2(pd)_{10}(py)_4(OCN)_7]_n$ have also been reported [23,24]. The use of such large polynuclear carboxylate building blocks offers additional possibilities for crystal engineering of interesting new materials with high porosity and could lead to attractive materials properties. This review provides an overview of our recent developments in exploring $Mn^{II,III}$-oxo and Fe^{III}-oxo pivalate and isobutyrate building blocks with stable $\{M_3(\mu_3\text{-}O)\}$, $\{M_4(\mu_3\text{-}O)_2\}$ (M = Mn, Fe), $\{Mn_6(\mu_4\text{-}O)_2\}$ or $\{Fe_6(\mu_3\text{-}O)_2\}$ cores in the formation of CCPs assemblies with an emphasis on the synthetic strategies and magnetic properties.

2. Oxo-Trinuclear Mn/Fe-Based CCPs

Trinuclear oxo-centered carboxylate coordination clusters of general composition $[M_3(\mu_3\text{-}O)(O_2CR)_6(L)_3]^{+/0}$ (where L = a neutral terminal ligand) are the most frequently used building blocks in the construction of CCPs. For assembling 1D oxo-trinuclear Mn/Fe CCPs, several synthetic strategies have been explored, e.g., using simple soluble metal salts or well-known pre-designed "basic carboxylate", e.g., μ_3-oxo trinuclear Mn/Fe carboxylate clusters. The combination of these starting materials with organic ligands, usually in "one-pot" syntheses at temperatures starting from room temperature and up to solvothermal conditions in different solvents, gave the expected CCPs. The first 1D CCP, $[Mn_3O(ac)_7(Hac)]_n$, which is composed of $[Mn_3(\mu_3\text{-}O)(ac)_6(Hac)]$ acetate clusters interlinked by acetate bridges, was reported by Hessel and Romers in 1969 [25], whereas Rentschler and Albores synthesized the first 1D CCP composed of $[Fe_3(\mu_3\text{-}O)(piv)_6(H_2O)]$pivalate clusters interlinked by dicyanamide (dca) bridges in 2008, $[Fe_3O(piv)_6(H_2O)(dca)]_n$ (where Hpiv = pivalic acid) [26].

Cronin, Kögerler et al. [27] suggested an effective route to assembling 1D CCPs through metal building block linkers in 2006. A helical $\{[(Fe_3O(aa)_6(H_2O))(MoO_4)(Fe_3O(aa)_6(H_2O)_2)] \cdot 2(MeCN) \cdot H_2O\}_n$ CCP (where Haa = acrylic acid) has been synthesized by linking the $[Fe_3O(aa)_6(H_2O)_3]^+$ cations with $[MoO_4]^{2-}$ dianions derived from $(Bu_4N)_2[Mo_6O_{19}]$ in MeCN. As an extension, Bu et al. [28] in 2015, introduced $[M(H_2O)_2(fa)_4]^{2-}$ formate building block linkers for connecting μ_3-oxo trinuclear neutral $[Fe_3O(fa)_7]$ formate clusters into $\{(NH_4)_2[Fe_3O(fa)_7]_2[M(H_2O)_2(fa)_4]\}_n$ CCPs (where Hfa = formic acid; M^{II} = Fe; Mn; Mg) with the formation of anionic double-strained chains.

The family of 1D Mn and Fe pivalate or isobutyrate CCPs (Table 1) has been generated by using simple metal carboxylates or employing pre-designed oxo-trinuclear building blocks in reactions [29,30]. Thus, mixing a hot ethanol solution of hexamethylenetetramine (hmta) with Mn^{II} isobutyrate in tetrahydrofuran yields the chain coordination polymer $\{[Mn_3O(is)_6(hmta)_2] \cdot EtOH\}_n$ (where His = isobutyric acid) (**1**) [29]. This CCP comprises neutral mixed-valent μ_3-oxo trinuclear $[Mn^{II}Mn^{III}_2O(is)_6]$ clusters bridged by hmta into a linear 1D chain as shown in Figure 1. To model its magnetic behavior, an approximation considered two trimers coupled through Mn^{III} and Mn^{II} ions (the Mn···Mn distances between clusters via hmta linkers are equal to 6.310 Å). For **1**, the authors reported significant

antiferromagnetic intracluster interactions between Mn spin centers with $2J_1$ = +32.5 K and $2J_2$ = −16.8 K, whereas the intercluster interactions through hmta spacers were found to be weakly ferromagnetic.
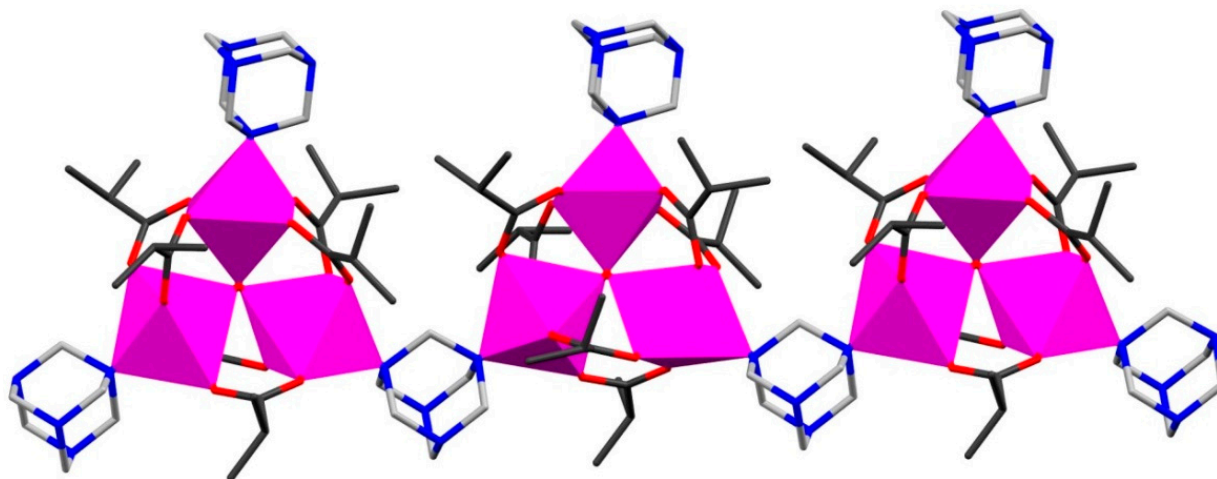

Figure 1. A linear 1D chain in {[Mn$_3$O(is)$_6$(hmta)$_2$]·EtOH}$_n$ (**1**) CCP [29]. H atoms and solvent (EtOH) molecules are omitted for clarity. Color codes: C, gray; N, blue; O red sticks. C atoms in carboxylates are shown as black sticks, and Mn atoms are shown as magenta coordination polyhedra.

Combining the different pre-designed μ$_3$-oxo trinuclear pivalate complexes such as [Fe$_3$O(piv)$_6$(H$_2$O)$_3$]piv·2(piv) and [Mn$_3$O(piv)$_6$(hmta)$_3$]·*n*-PrOH in one-pot reactions with the same spacer (hmta) lead to the formation of heteronuclear Fe/Mn-oxo 1D CCPs [30]. The solvothermal reaction of these precursors in MeCN at 120 °C for 4 h gave a heterometallic chain polymer {[Fe$_2$MnO(piv)$_6$(hmta)$_2$]·0.5(MeCN)}$_n$ (**2**), while refluxing in *n*-hexane resulted in the solvated heterometallic chain polymer {[Fe$_2$MnO(piv)$_6$(hmta)$_2$]·Hpiv·*n*-hexane}$_n$ (**3**). Magnetic studies of **2** and **3** indicated dominant antiferromagnetic interactions between the metal centers with significant intercluster interaction through hmta spacer with the following exchange parameters: $J_{\text{Mn}^{\text{II}}-\text{Fe}^{\text{III}}}$ = −17.4 cm^{-1} and $J_{\text{Fe}^{\text{III}}-\text{Fe}^{\text{III}}}$ = −43.7 cm^{-1} for **2**; and $J_{\text{Mn}^{\text{II}}-\text{Fe}^{\text{III}}}$ = −23.8 cm^{-1} and $J_{\text{Fe}^{\text{III}}-\text{Fe}^{\text{III}}}$ = −53.4 cm^{-1} for **3**. All intercluster exchange interactions were modeled using a molecular field model approximation to give λ_{mf} = −0.219 mol cm^{-3} (**2**) and λ_{mf} = −0.096 mol cm^{-3} (**3**) [30].

In comparison to Baca and Kögerler's approach, Kolotilov et al. [31–34] employed already preformed oxo-centered heterometallic trinuclear [Fe$_2$MO(piv)$_6$(Hpiv)$_3$] (M$^{\text{II}}$ = Co, Ni) pivalates to isolate a series of heterometallic 1D CCPs formulated as {[Fe$_2$CoO(piv)$_6$(bpe)]·0.5(bpe)}$_n$, [Fe$_2$NiO(piv)$_6$(bpp)(dmf)]$_n$, {[Fe$_2$NiO(piv)$_6$(pnp)(dmso)] ·2.5(dmso)}$_n$, [Fe$_2$NiO(piv)$_6$(pnp)(H$_2$O)]$_n$, {[(Fe$_2$NiO(piv)$_6$)$_4$(Et-4-ppp)$_6$]·3(def)}$_n$, and [Fe$_2$NiO(piv)$_6$(bpt)$_{1.5}$]$_n$ (where bpe = 1,2-bis(4-pyridyl)ethylene, bpp = 1,3-bis(4-pyridyl)propane, pnp = 2,6-bis(4-pyridyl)-4-(1-naphtyl)pyridine, Et-4-ppp = 4-(*N,N*-diethylamino)phenyl-bis-2,6-(4-pyridyl)pyridine, bpt = 3,6-bis(3-pyridyl)-1, 2,4,5-tetrazine).

The presence of three potential donor metal sites in the oxo-centered trinuclear carboxylate species makes this building block very attractive and useful for the construction of 2D CCPs. The first homometallic 2D {[Fe$_3$O(ac)$_6$(H$_2$O)$_3$][Fe$_3$O(ac)$_{7.5}$]$_2$·7(H$_2$O)}$_n$ cluster-based layer has been prepared by Long and coworkers [35] in 2007 from the reaction of a trinuclear iron acetate, [Fe$_3$O(ac)$_6$(H$_2$O)$_3$]Cl·6H$_2$O, FeCl$_3$·4H$_2$O and sodium acetate in MeCN/water solution at room temperature in 4 months. The main feature of it is the formation of the "star" anionic layer of acetate-bridged [Fe$_3$O(ac)$_6$]$^+$ clusters that contain in its channels cationic guest-trimer [Fe$_3$O(ac)$_6$(H$_2$O)$_3$]$^+$ clusters. In 2009, Pavlishchuk et al. [36] reacted simple salt precursors, namely iron(III) nitrate nonahydrate and manganese(II) nitrate hexahydrate, with formic acid under heating to isolate the first heterometallic 2D CCP

$\{[Fe_3O(fa)_6][Mn(fa)_3(H_2O)_3]\cdot3.5(Hfa)\}_n$. This compound consists of trinuclear $[Fe_3O(fa)_6]^+$ units linked by mononuclear $[Mn(fa)_3(H_2O)_3]^-$ bridges into 2D honeycomb layers.

By refluxing the presynthesized pivalate complex compounds $[Mn_3O(piv)_6(hmta)_3]\cdot n$-PrOH and $[Fe_3O(piv)_6(H_2O)_3]piv\cdot2(Hpiv)$ in a hot toluene solution for 6 h, the new 2D heterometallic coordination polymer $\{[Fe_2MnO(piv)_6(hmta)_{1.5}]\cdot toluene\}_n$ (**4**) can be prepared [30]. In contrast to the above-mentioned 1D CCPs (**1–3**), in **4** hmta ligands, connect neighboring heterometallic $\{[Fe_2Mn(\mu_3-O)(piv)_6]$ pivalate clusters into a 2D corrugated layer as shown in Figure 2. The formed framework accommodates guest toluene molecules. In **4**, the exchange interactions between Mn^{II} and Fe^{III} were found to be antiferromagnetic ($J_{Mn^{II}-Fe^{III}} = -13.3$ cm^{-1}; $J_{Fe^{III}-Fe^{III}} = -35.4$ cm^{-1}), with significant intercluster interactions through hmta ($\lambda_{mf} = -0.051$ mol cm^{-3}). A series of 2D heterometallic pivalate CCPs built from $[Fe_2MO(piv)_6]$ (M^{II} = Co, Ni) clusters bridged by different polydentate polypyridyl-type linkers has also been reported by other groups [31,36–38].

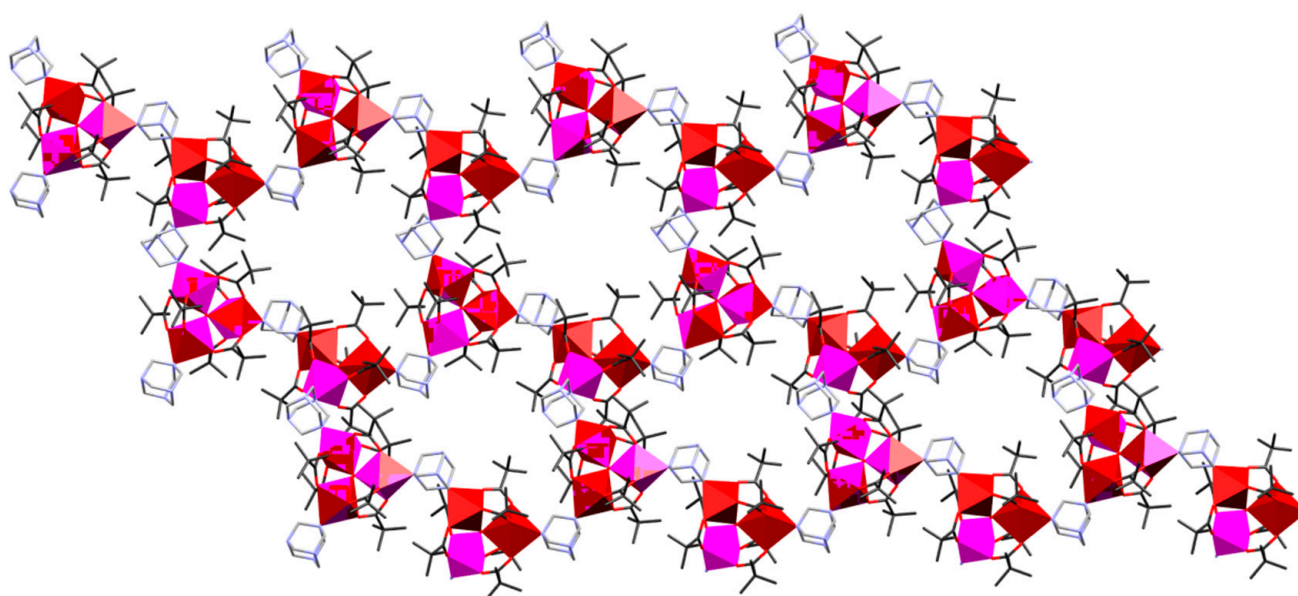**Figure 2.** A heterometallic 2D layer in $\{[Fe_2MnO(piv)_6(hmta)_{1.5}]\cdot toluene\}_n$ (**4**) CCP [30]. H atoms and solvent toluene molecules are omitted for clarity. Color codes: C, gray; N, blue; O red sticks and Fe/Mn atoms are shown as brown/magenta coordination polyhedra. C atoms in carboxylates are shown as black sticks.

In 2014, Baca and Kögerler et al. [39] reported the first 3D cluster-based coordination polymers, $\{[Fe_3O(piv)_6(4,4'-bpy)_{1.5}](OH)\cdot0.75(dcm)\cdot8(H_2O)\}_n$ (**5**) and $[Fe_2CoO(piv)_6(bpe)_{0.5}(pyz)]_n$ (**6**). Relative to the 1D and 2D CCPs, 3D structures based on Mn/Fe trinuclear oxo-clusters are rare: up to now, only three compounds were reported [39,40]. CCPs **5** and **6** consist of μ_3-oxo-centered cationic homometallic $[Fe^{III}_3(\mu_3-O)(piv)_6]^+$ or neutral heterometallic $[Fe^{III}_2Co^{II}(\mu_3-O)(piv)_6]$ coordination clusters bridged by different *N,N'*-donor ligands: 4,4'-bipyridine (4,4'-bpy) in case of **5**, and 1,2'-bis(4-pyridyl)ethylene (bpe) and pyrazine (pyz) in case of **6**. They were prepared in a "one-pot" solvothermal reaction in dichloromethane from $[Fe_6O_2(OH)_2(piv)_{12}]$ and organic spacers, and, additionally, cobalt(II) pivalate was added in **6**. It is worth noting that the mutual arrangement of three-connected $[M_3(\mu_3-O)(piv)_6]$ nodes linked by a linear spacer determines the topology of the final CCPs. Here, neighboring μ_3-oxo trinuclear clusters are mutually perpendicular, and the pair of clusters may be regarded as a pseudo-tetrahedral four-connected binodal building block, and as a result, 3D porous networks are formed. A 6-fold interpenetrated network with rare (8.3)-c (**etc**) topology can be observed in **5**, and a three-fold interpenetrated network with (10.3)-b (**ths**) topology in **6** (Figure 3). Magnetic studies of **5** and **6** point to both ferro- and antiferromagnetic intra- and intercluster exchange interactions between the isotropic Fe^{III} and/or the strongly anisotropic (octahedrally coordinated) Co^{II}

spin centers. In particular, the $\chi_m T$ value of 7.54 cm³ K mol⁻¹ at 290 K, significantly smaller than the expected spin-only value of 13.1 cm³ K mol⁻¹ for three isolated $S = 5/2$ centers ($g_{iso} = 2.0$) for **5**, indicates dominant antiferromagnetic exchange interactions mediated by the central μ_3-O within {Fe₃(μ_3-O)} unit ($J_1 = -0.1$ cm⁻¹ and $J_2 = -27.0$ cm⁻¹) and the 4,4′-bpy bridges ($\lambda_{mf} = -0.609$ mol cm⁻³, the Fe⋯Fe distances via 4,4′-bpy are equal to 11.347 and 11.380 Å). For **6**, both contributions of the orbital momentum of Co^{II} center in {Fe₂Co} unit and intracluster (ferromagnetic) and intercluster (ferromagnetic) coupling within {Fe₂Co} triangular unit and between them have been considered via the magnetochemical computational framework CONDON [41,42]. The exchange interaction parameters are $J_{Co^{II}-Fe^{III}} = +55.0$ cm⁻¹, $J_{Fe^{III}-Fe^{III}} = -122.0$ cm⁻¹ and $\lambda_{mf} = +1.163$ mol cm⁻³ (through the pyz ligand the M⋯M distances are 7.096 and 7.142 Å, and through the bpe spacer these distances equal 13.603 Å). Subsequently, a 3D CCP, {[NH₄]₂[Fe₉O₃(ac)₂₃(H₂O)]}ₙ, with triangular [Fe₃(μ_3-O)(ac)₆]⁺ cations and acetate as linkers between the units has been reported by Bu et al. [40]. Its structure exhibits a 4-fold interpenetrating 3D network with a rare **eta-c4** net topology.
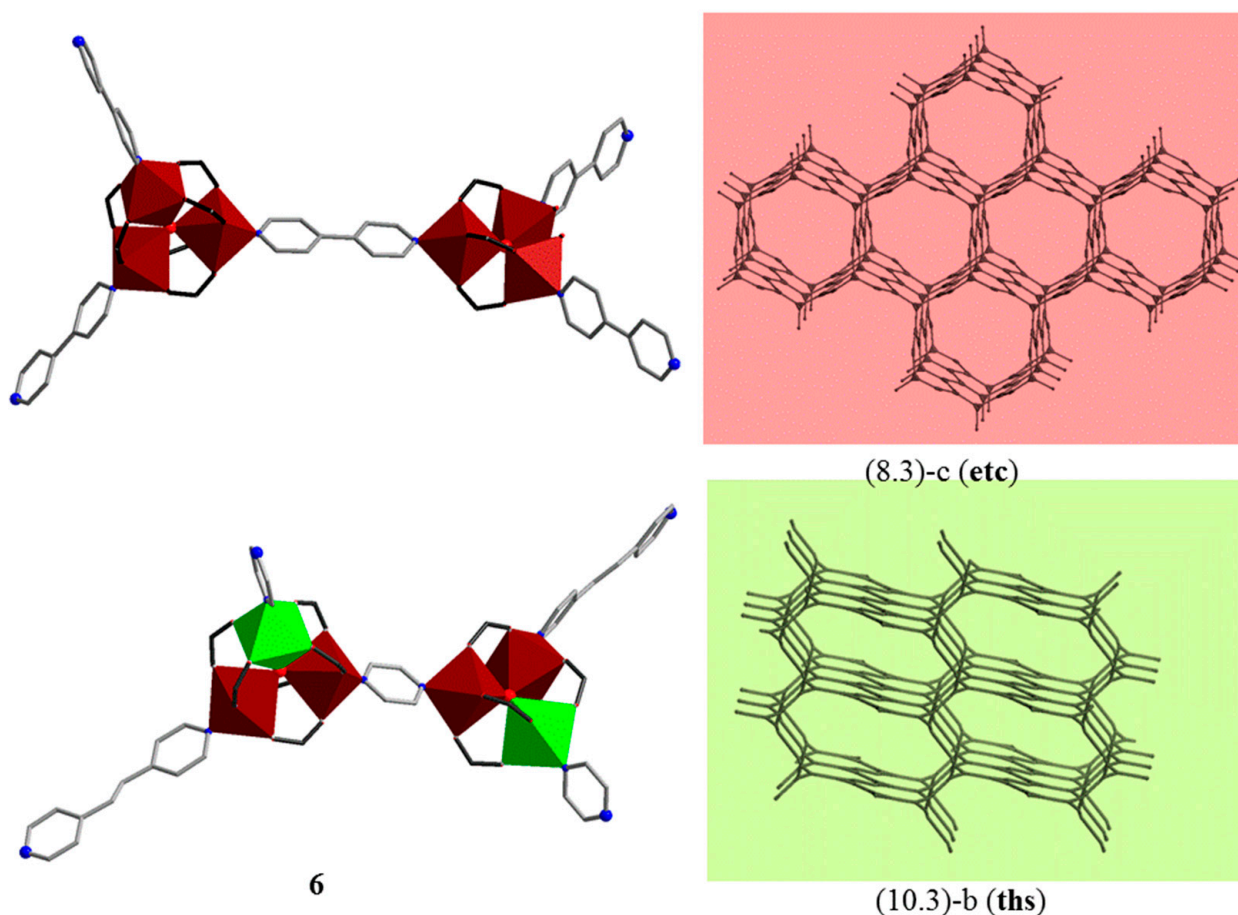
Figure 3. 3D layers in {[Fe₃O(piv)₆(4,4′-bpy)₁.₅](OH)·0.75(dcm)·8(H₂O)}ₙ (**5**) and [Fe₂CoO(piv)₆(bpe)₀.₅(pyz)]ₙ (**6**) CCPs [39]. H atoms and CMe₃ groups are omitted for clarity. Color codes: Fe, brown; Co, green coordination polyhedra; C, gray sticks; N, blue; O red spheres. C atoms in carboxylates are shown as black sticks.

3. Oxo-Tetranuclear Mn/Fe-Based CCPs

Oxo-tetranuclear Mn and Fe carboxylate complexes often called "butterfly" clusters, possess a well-known {M₄(μ_3-O)₂} core. The core comprises an inner "body" metal atoms doubly bridged by two μ_3-oxo atoms, connected outwards to the remaining "wing" metal atoms. The core can also be considered as two edge-sharing {M₃(μ_3-O)} triangular units. Although the core can be considered as potential [M₄O₂(O₂CR)ₓ(L)ᵧ] nodes, only 1D

CCPs from tetranuclear {Mn$_4$(μ_3-O)$_2$} and {Fe$_4$(μ_3-O)$_2$} carboxylate oxo-clusters have been reported thus far [29,43–45].

Christou and coworkers [44] first reported a 1D {Mn$_4$O$_2$}-based benzoate-bridged CCP formulated as [Mn$_4$O$_2$(ba)$_6$(dbm)$_2$(4,4′-bpy)]$_n$ (where Hba = benzoic acid; dbm = dibenzoylmethane) in 1994. Since then, only a few more {Mn$_4$O$_2$}-CCPs were reported. A 1D CCP, [Mn$_4$O$_2$(is)$_6$(bpm)(EtOH)$_4$]$_n$ (**7**), composed of mixed-valence tetranuclear [Mn$^{II}_2$Mn$^{III}_2$(μ_3-O)$_2$(is)$_6$(EtOH)$_4$] isobutyrate building blocks bridged by 2,2′-bipyrimidine (bpm) linkers (Figure 4), has been identified in 2008 [29] (Table 1). The addition of an ethanol solution of bpm to Mn(II) isobutyrate in tetrahydrofuran solution directly results in the formation of **7**. The temperature dependence of χT in **7** indicates dominant antiferromagnetic interactions inside the {Mn$_4$} units with a value of 13.46 cm^3 K mol^{-1} at 300 K that is close to the value expected for an uncoupled {Mn$^{II}_2$Mn$^{III}_2$} system (χT = 14.75 cm^3 K mol^{-1} for g = 2.00).
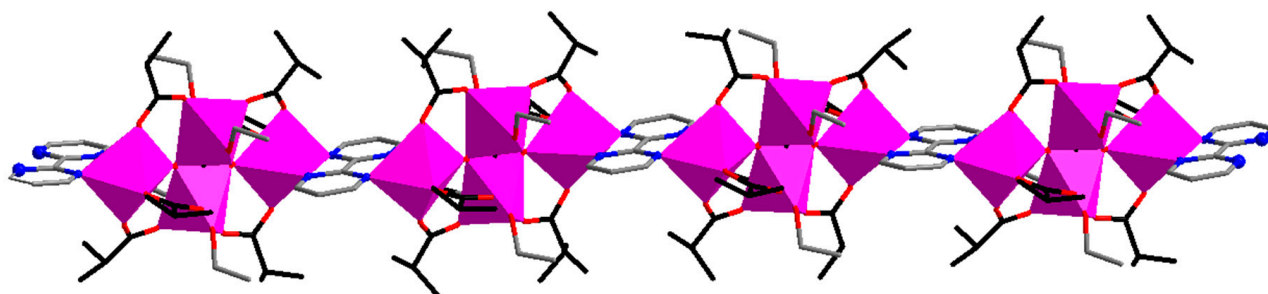
Figure 4. A linear 1D chain in [Mn$_4$O$_2$(is)$_6$(bpm)(EtOH)$_4$]$_n$ (**7**) CCP [29]. H atoms are omitted for clarity. Color codes: C, gray; O red sticks; N, blue spheres. C atoms in carboxylates are shown as black sticks, and Mn atoms are shown as magenta coordination polyhedra.

The first tetranuclear {Fe$_4$O$_2$}-based coordination polymer [Fe$_4$O$_2$(piv)$_8$(hmta)]$_n$ (**8**) reported in 2011 by Baca and coworkers [43] was isolated from the reaction of the μ_3-oxo trinuclear pivalate complex [Fe$_3$O(piv)$_6$(H$_2$O)$_3$]piv·2(Hpiv) with hmta in MeCN. In **8**, tetranuclear [Fe$_4$(μ_3-O)$_2$(piv)$_8$] clusters are bridged by hmta ligands forming zigzag chains (Figure 5). Magnetochemical analysis of the {Fe$_4$} butterfly-like CCP **8** indicates that the interactions between body-body Fe^{III} ions were antiferromagnetic with a least-squares fit yielding J_{bb} = −22 cm^{-1}.

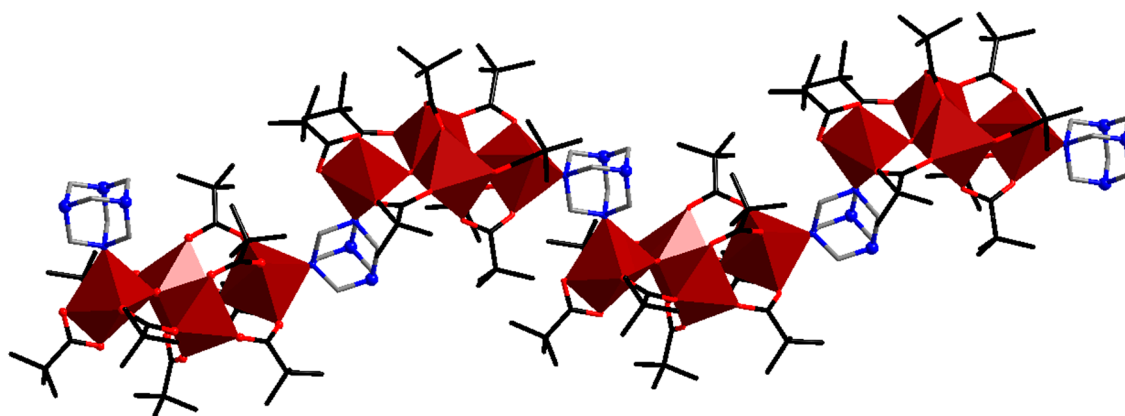**Figure 5.** A zigzag 1D chain in [Fe$_4$O$_2$(piv)$_8$(hmta)]$_n$ (**8**) CCP [43]. H atoms are omitted for clarity. Color codes: C, gray; O red sticks; N, blue spheres. C atoms in carboxylates are shown as black sticks, and Fe atoms are shown as brown coordination polyhedra.

4. Oxo-Hexanuclear Mn/Fe CCPs

One of the fascinating Mn oxo-carboxylate clusters used as building blocks in the construction of CCPs are hexanuclear clusters $[Mn_6O_2(O_2CR)_{10}(L)_4]$ (where L = neutral monodentate ligand) with a central $\{Mn_6O_2\}$ core. The central mixed-valence $[Mn^{II}_4Mn^{III}_2(\mu_4\text{-}O)_2]^{10+}$ core consists of six Mn centers, two Mn^{III} and four Mn^{II} ions, arranged as two edge-sharing flattened Mn_4 tetrahedra, with a $\mu_4\text{-}O^{2-}$ ion in the center of each tetrahedron. Peripheral ligation is provided by bridging carboxylate groups. Within the core, two central Mn atoms are in the formal oxidation state +3, and the four terminal Mn atoms are in the lower oxidation state +2. Careful choice of appropriate exo-bidentate spacer ligands with the selection of starting precursors and media solution allowed interlinking the $\{Mn_6(\mu_4\text{-}O)_2\}$ oxo-clusters into 1D coordination polymeric chains, 2D layers or 3D frameworks.

The first 1D coordination polymers $[Mn_6O_2(piv)_{10}(Hpiv)_2(4,4'\text{-}bpy)]_n$ based on $\{Mn_6O_2\}$ pivalate building blocks bridged by 4,4'-bipyridine (4,4'-bpy) were obtained by Yamashita et al. in 2002 [46]. Assembling of $\{Mn_6O_2\}$ building clusters into coordination networks by shorter linkers was executed later. In 2008, Chen's group isolated the propionate-bridged $\{[Mn_6O_2(O_2CEt)_{10}(H_2O)_4]\cdot2(EtCO_2H)\}_n$ CCP [47] and Tasiopoulos's group in 2010 reported the acetato-bridged $\{[Mn_6O_2(ac)_{10}(H_2O)_4]\cdot2.5(H_2O)\}_n$ CCP [48].

A new series of 1D CCPs based on the $\{Mn_6(\mu_4\text{-}O)_2\}$ pivalate and isobutyrate clusters, namely $\{[Mn_6O_2(piv)_{10}(Hpiv)(EtOH)(na)]\cdot EtOH\cdot H_2O\}_n$ (**9**), $[Mn_6O_2(piv)_{10}(Hpiv)_2(en)]_n$ (**10**), $\{[Mn_6O_2(is)_{10}(pyz)_3]\cdot2(H_2O)\}_n$ (**11**), $[Mn_6O_2(is)_{10}(pyz)(MeOH)_2]_n$ (**12**), and $\{[Mn_6O_2(is)_{10}(pyz)_{1.5}(H_2O)]\cdot0.5(H_2O)\}_n$ (**13**), $\{[Mn_6O_2(is)_{10}(His)(EtOH)(bpea)]\cdot His\}_n$ (**14**), (where na = nicotinamide, en = ethyl nicotinate, pyz = pyrazine, bpea = 1,2-bis(4-pyridyl)ethane) have been reported [49,50] (Table 1). All CCPs, except **10**, have been prepared by the reaction of simple Mn^{II} pivalate or isobutyrate salts with the appropriate bridging ligand in different solvents: MeCN solution in case of **9** and **13**, MeCN/EtOH (1:1 *v:v*) solution for **11**, MeCN/MeOH (1:1 *v:v*) solution for **12**, and thf/EtOH solution (1:1 *v:v*) for **14**. CCP **10** was isolated from the reaction of $[Mn_6O_2(O_2CCMe_3)_{10}(thf)_4]$ with ethyl nicotinate in decane. The spacer length and spacer flexibility have an important effect on the complex structures in these systems. The shorter pyz ligand connects neighboring $\{Mn_6(\mu_4\text{-}O)_2\}$ clusters to form 1D zigzag chains in **11** (intercluster Mn⋯Mn: 7.288 Å), linear chains in **12** (intercluster Mn⋯Mn: 7.443 Å), and ladder-like chains in **13** (intercluster Mn⋯Mn: 7.415 and 7.480 Å). The na group links the $\{Mn_6(\mu_4\text{-}O)_2\}$ clusters into linear chains in **10** (intercluster Mn⋯Mn: 8.690 Å), and finally, bpea bridges the $\{Mn_6(\mu_4\text{-}O)_2\}$ clusters (intercluster Mn⋯Mn: 9.239 Å) in a unique meander-type chain as shown in Figure 6 in **14**. Magnetochemical analysis of **9**, **11**, and **14** finds significant intercluster antiferromagnetic interactions through the shorter pyz and na linkers ($\lambda_{mf} = -1.131$ mol cm^{-3} (**9**), -1.508 mol cm^{-3} (**11**)), and the intercluster interaction via long bpea is negligible in **14**. Within $\{Mn_6\}$ fragments, the intracluster interactions are antiferromagnetic with the best-fit parameters $J_1 = -1.61$ cm^{-1}, $J_2 = J_3 = -0.89$ cm^{-1} and $J_4 = -1.23$ cm^{-1}. Here J_1 is the exchange coupling constant describing the nearest-neighbor Mn^{III}⋯Mn^{III} interactions through two μ_4-O centers, $J_2 = J_3$—for Mn^{III}⋯Mn^{II} interactions mediated by μ_4-O and μ_3-O centers and a carboxylate (J_2) or a μ_4-O center and a carboxylate (J_3), and J_4—for Mn^{II}⋯Mn^{II} interactions via a μ_4-O center and a carboxylate group. We note that Ovcharenko et al. [51] linked the polynuclear $\{Mn_6\}$ pivalate fragments by nitronyl nitroxide radical (2,4,4,5,5-pentamethyl-4,5-dihydro-1*H*-imidazolyl-3-oxide-1-oxyl (NIT-Me) to isolate 1D molecular magnet $\{[Mn_6O_2(piv)_{10}(thf)_2(NIT\text{-}Me)][Mn_6O_2(piv)_{10}(thf)_2(dcm)(NIT\text{-}Me)]\}_n$ with T_c = 3.5 K.
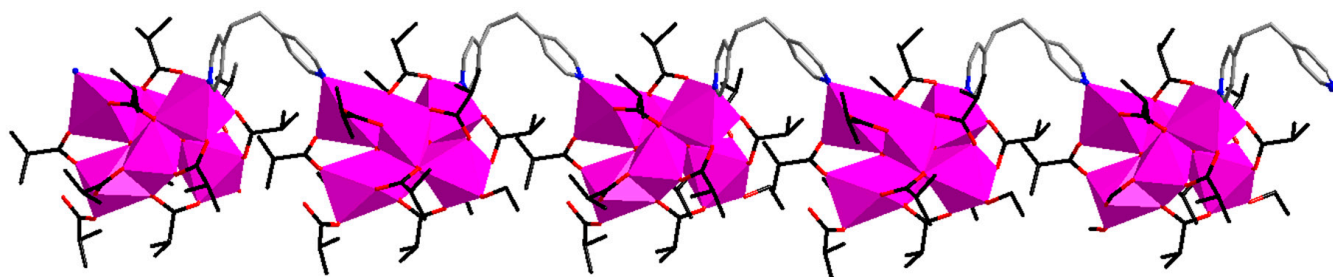
Figure 6. 1D meander-like chain in $\{[Mn_6O_2(is)_{10}(His)(EtOH)(bpea)]\cdot His\}_n$ (**14**) CCP [49]. H atoms and solvate His are omitted for clarity. Color codes: C, gray; O red sticks; N, blue spheres. C atoms in carboxylates are shown as black sticks, and Mn atoms are shown as magenta coordination polyhedra.

In contrast to hexanuclear $\{Mn_6(\mu_4\text{-}O)_2\}$ building blocks, the use of hexanuclear $\{Fe_6(\mu_3\text{-}O)_2\}$ building blocks in the design of CCPs is fairly scarce. Until now, only two such compounds have been published [52]. 1D zigzag chain coordination polymers $[Fe_6O_2(O_2CH_2)(piv)_{12}(diox)]_n$ (**15**) (Figure 7) and $[Fe_6O_2(O_2CH_2)(piv)_{12}(4,4'\text{-}bpy)]_n$ (**16**) (where diox = 1,4-dioxane; 4,4'-bpy = 4,4'-bipyridine) have been prepared from smaller pre-designed μ_3-oxo trinuclear $[Fe_3O(piv)_6(H_2O)_3]piv\cdot 2(Hpiv)$ or hexanuclear $[Fe_6O_2(OH)_2(piv)_{12}]$ species by slow diffusion of MeCN into its solution in 1,4-dioxane (**15**) or heating starting $[Fe_6O_2(OH)_2(piv)_{12}]$ and 4,4'-bpy in $CH_2Cl_2/MeCN$ (**16**). Although the $\{Fe_6\}$ building blocks in **15** and **16** show the general similarity (Fe$\cdots$Fe distances differ less than 0.015 Å from their averages), the observed magnetic low-field susceptibility displays strong differences, mainly from inter-$\{Fe_6\}$ cluster coupling mediated either by the diox (closest Fe$\cdots$Fe contact: 7.171 Å) or the 4,4'-bpy (11.39 Å) linkers. The magnetism of the $[Fe_6O_2(O_2CH_2)(piv)_{12}]$ clusters was modeled assuming that the $\{Fe_6\}$ cluster consists of two identical isosceles $Fe_3(\mu_3\text{-}O)$ triangles with three exchange energies (J_{1-3}) between the spin-only ($S = 5/2$; $^6A_{1g}$) Fe^{III} centers. CCPs **15** and **16** exhibit dominant antiferromagnetic interactions among the Fe^{III} ions within the $\{Fe_6\}$ clusters (J_1 and J_2 between Fe^{III} ions in $\{Fe_3O\}$ triangles and J_3—between the triangles) and possible antiferromagnetic intercluster interaction (λ_{mf}) with the best-fit $J_1 = -30.82$ cm^{-1}, $J_2 = -14.43$ cm^{-1}, $J_3 = -11.75$ cm^{-1} and $\lambda_{mf} = -11.6$ mol cm^{-3} for **15**, and $J_1 = -32.77$ cm^{-1}, $J_2 = -14.11$ cm^{-1}, $J_3 = -10.57$ cm^{-1} and $\lambda_{mf} = -0.12$ mol cm^{-3} for **16**.
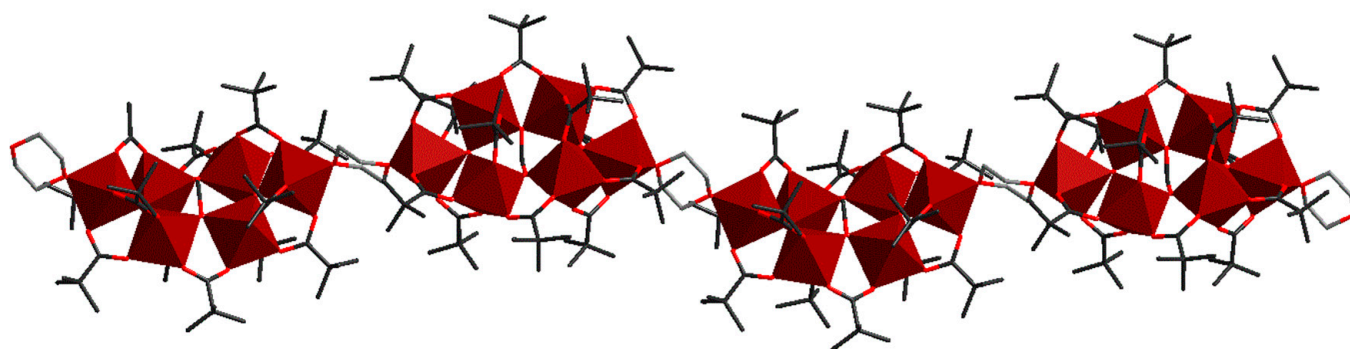
Figure 7. A 1D chain in $[Fe_6O_2(O_2CH_2)(piv)_{12}(diox)]_n$ (**15**) [52]. H atoms are omitted for clarity. Color codes: C, gray; O red sticks. C atoms in carboxylates are shown as black sticks, and Fe atoms are shown as brown coordination polyhedra.

Using isonicotinamide (ina), Ovcharenko and co-workers in 2013 [53] prepared the first 2D pivalate CCPs based on a $\{Mn_6O_2\}$ carboxylate motif, $\{[Mn_6O_2(piv)_{10}(ina)_2]\cdot 3(Me_2CO)\}_n$ and $\{[Mn_6O_2(piv)_{10}(ina)_2]\cdot 2(EtOAc)\}_n$. Employing the same ina spacer, an anhydrous $[Mn_6O_2(piv)_{10}(ina)_2]_n$ (**17**) CCP was obtained from the simple manganese(II) pivalate and ina in a mixture of MeCN/EtOH in 2014 [54] (Figure 8a). Similar to Ovcharenko's CCPs, $\{Mn_6\}$ pivalate clusters are bridged via ina spacer ligands in a 2D polymeric (4,4) layer with a Mn$^{II}\cdots$Mn^{II} distance of 9.279 and 9.357 Å. Two other 2D CCPs $\{[Mn_6O_2(piv)_{10}(adt$-

4)$_2$]·2(thf)}$_n$ (**18**) and {[Mn$_6$O$_2$(is)$_{10}$(adt-4)$_2$]·thf·3(EtOH)}$_n$ (**19**) were prepared from the reaction of a simple [Mn(piv)$_2$] salt (**18**) or a hexanuclear [Mn$_6$(is)$_{12}$(His)$_6$] isobutyrate cluster (**19**) and the bent, semi-rigid *N,N′*-donor aldrithiol (adt-4) spacer ligands in thf. Interestingly, four semi-rigid aldrithiol ligands joint the adjacent {Mn$_6$} clusters in a different way: if in **18,** a 2D polymeric layer with grid topology is formed, in **19,** an intriguing bilayer framework occurs (Figure 8b). In **19**, a pair of adt-4 ligands connect the neighboring {Mn$_6$} isobutyrate clusters to form linear chains with a Mn^{II}···Mn^{II} distance of 10.537 Å between neighboring {Mn$_6$} units. Another pair of adt-4 ligands double cross-link neighboring {Mn$_6$} clusters from differently oriented chains (Mn^{II}···Mn^{II}: 10.873 Å) resulting in a rare 2D bilayer (Figure 8b). Thus, the hexanuclear [Mn$_6$O$_2$(is)$_{10}$] isobutyrate clusters here serve as 3-connected T-shaped nodes and represent the first example of a CCP with such bilayer topology. Magnetic susceptibility measurements for **17–19** indicate a net of antiferromagnetic intracluster and intercluster exchange interactions, resulting in singlet ground states. An intracluster coupling scheme defines four types of exchange energies in {Mn$_6$} clusters with the best-fit $J_{Mn^{III}-Mn^{III}} = -15.4$ cm^{-1}, $J_{Mn^{II}-Mn^{II}} = -1.9$ cm^{-1}, $J_{Mn^{III}-Mn^{II}} = -2.8$ cm^{-1}, and $J_{Mn^{II}-Mn^{II},ext} = +5.5$ cm^{-1}, resulting in an overall $S = 0$ ground state for each {Mn$_6$} cluster. The molecular field parameter results in $\lambda = -1.1$ mol cm^{-3}, indicating antiferromagnetic intercluster coupling.

Table 1. Cluster-based coordination polymers (CCPs) built up from Fe/Mn-oxo pivalates and isobutyrates.

Code	Formulae	Oxo Building Block	Linker [1]	Dimensionality	Refs
1	{[Mn$_3$O(is)$_6$(hmta)$_2$]·EtOH}$_n$	{Mn$^{III}_2$Mn^{II}O}	hmta	1D	[29]
2	{[Fe$_2$MnO(piv)$_6$(hmta)$_2$]·0.5(MeCN)}$_n$	{Fe$^{III}_2$Mn^{II}O}	hmta	1D	[30]
3	{[Fe$_2$MnO(piv)$_6$(hmta)$_2$]·Hpiv·*n*-hexane}$_n$	{Fe$^{III}_2$Mn^{II}O}	hmta	1D	[30]
4	{[Fe$_2$MnO(piv)$_6$(hmta)$_{1.5}$]·toluene}$_n$	{Fe$^{III}_2$Mn^{II}O}	hmta	2D	[30]
5	{[Fe$_3$O(piv)$_6$(4,4′-bpy)$_{1.5}$](OH)·0.75(dcm)·8(H$_2$O)}$_n$	{Fe$^{III}_3$O}	4,4′-bpy	3D	[39]
6	[Fe$_2$CoO(piv)$_6$(bpe)$_{0.5}$(pyz)]$_n$	{Fe$^{III}_2$Co^{II}O}	bpe, pyz	3D	[39]
7	[Mn$_4$O$_2$(is)$_6$(bpm)(EtOH)$_4$]$_n$	{Mn$^{III}_2$Mn$^{II}_2$O$_2$}	bpm	1D	[29]
8	[Fe$_4$O$_2$(piv)$_8$(hmta)]$_n$	{Fe$^{III}_4$O$_2$}	hmta	1D	[43]
9	{[Mn$_6$O$_2$(piv)$_{10}$(Hpiv)(EtOH)(na)]·EtOH·H$_2$O}$_n$	{Mn$^{III}_2$Mn$^{II}_4$O$_2$}	na	1D	[49]
10	[Mn$_6$O$_2$(piv)$_{10}$(Hpiv)$_2$(en)]$_n$	{Mn$^{III}_2$Mn$^{II}_4$O$_2$}	en	1D	[50]
11	{[Mn$_6$O$_2$(is)$_{10}$(pyz)$_3$]·2(H$_2$O)}$_n$	{Mn$^{III}_2$Mn$^{II}_4$O$_2$}	pyz	1D	[49]
12	[Mn$_6$O$_2$(is)$_{10}$(pyz)(MeOH)$_2$]$_n$	{Mn$^{III}_2$Mn$^{II}_4$O$_2$}	pyz	1D	[50]
13	{[Mn$_6$O$_2$(is)$_{10}$(pyz)$_{1.5}$(H$_2$O)]·0.5(H$_2$O)}$_n$	{Mn$^{III}_2$Mn$^{II}_4$O$_2$}	pyz	1D	[50]
14	{[Mn$_6$O$_2$(is)$_{10}$(His)(EtOH)(bpea)]·His}$_n$	{Mn$^{III}_2$Mn$^{II}_4$O$_2$}	bpea	1D	[49]
15	[Fe$_6$O$_2$(O$_2$CH$_2$)(piv)$_{12}$(diox)]$_n$	{Fe$^{III}_6$O$_2$}	diox	1D	[52]
16	[Fe$_6$O$_2$(O$_2$CH$_2$)(piv)$_{12}$(4,4′-bpy)]$_n$	{Fe$^{III}_6$O$_2$}	4,4′-bpy	1D	[52]
17	[Mn$_6$O$_2$(piv)$_{10}$(ina)$_2$]$_n$	{Mn$^{III}_2$Mn$^{II}_4$O$_2$}	ina	2D	[54]
18	{[Mn$_6$O$_2$(piv)$_{10}$(adt-4)$_2$]·2(thf)}$_n$	{Mn$^{III}_2$Mn$^{II}_4$O$_2$}	adt-4	2D	[54]
19	{[Mn$_6$O$_2$(is)$_{10}$(adt-4)$_2$]·thf·3(EtOH)}$_n$	{Mn$^{III}_2$Mn$^{II}_4$O$_2$}	adt-4	2D	[54]

[1] hmta = hexamethylenetetramine; 4,4′-bpy = 4,4′-bipyridine; bpe = 1,2′-bis(4-pyridyl)ethylene; pyz = pyrazine; bpm = 2,2′-bipyrimidine; na = nicotinamide; en = ethyl nicotinate; bpea = 1,2-bis(4-pyridiyl)ethane; diox = 1,4-dioxane; ina = isonicotinamide; adt-4 = aldrithiol.
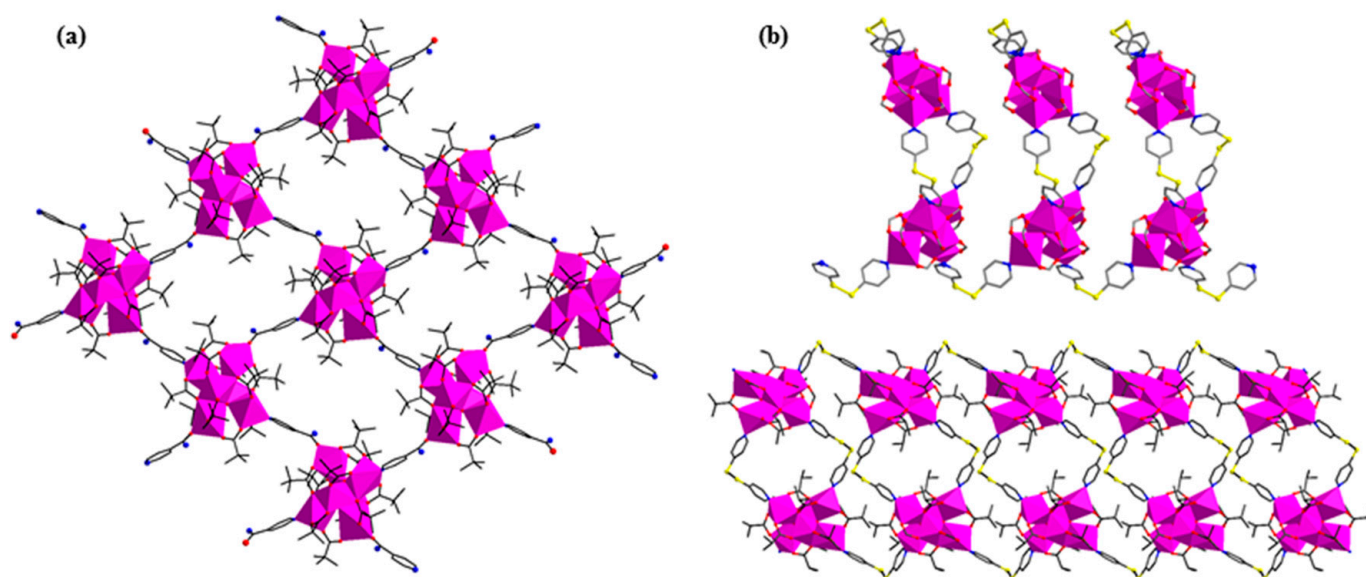
Figure 8. (**a**) A 2D (4,4) layer in $[Mn_6O_2(piv)_{10}(ina)_2]_n$ (**17**) CCP. (**b**) A rare T-shaped bilayer in $\{[Mn_6O_2(is)_{10}(adt-4)_2]\cdot thf\cdot 3(EtOH)\}_n$ (**19**) CCP [54]. H atoms and solvent molecules are omitted for clarity. Color codes: C, gray sticks; O red; N, blue; S, yellow spheres. Mn atoms are shown as magenta coordination polyhedra.

The first example of 3D oxo-hexanuclear $\{Mn_6\}$ pivalate CCP appeared in 2004 when Ovcharenko et al. reported a honeycomb $[Mn_6O_2(piv)_{10}(NIT-Me)_2]_n$ motif [51]. The second 3D oxo-hexanuclear $[Mn_6O_2(O_2CCH_2C_6H_5)_{10}(pyz)_2]_n$ CCP was synthesized in 2012 by Ghosh and coworkers who used pyrazine (pyz) linker to connect $\{Mn_6\}$ phenyl acetate clusters into a diamond-like framework with a (6,4) topology [55].

5. Conclusions

Polynuclear $Mn^{II,III}/Fe^{III}$-oxo pivalate and isobutyrate clusters recommend themselves as extremely versatile building blocks. Their ancillary coordinating ligands are sufficiently flexible to allow for the formation of a wide variety of structurally diverse and topologically interesting CCPs. Using metal-containing carboxylate building units ranging from trinuclear $\{M_3O\}$ to hexanuclear $\{M_6O_2\}$ cores, 1D, 2D and 3D CCPs have successfully been isolated. We note that this robust and versatile materials platform, based on oxo-carboxylate coordination cluster structures, is particularly attractive in the field of "intelligent" multifunctional materials, including magnetic sensors and spintronic devices since the targeted molecular systems allow for a combination of their intrinsic stability and physical quantum characteristics with unique structural features. However, despite their prominent role at the forefront of magnetic materials research, significant efforts remain focused on developing and understanding their complex magnetic characteristics as well as establishing magneto-structural correlations for these systems.

Conflicts of Interest: The authors declare no conflict of interest.

References

1. Zhang, W.-X.; Liao, P.-Q.; Lin, R.-B.; Wei, Y.-S.; Zeng, M.-H.; Chen, X.-M. Metal cluster-based functional porous coordination polymers. *Coord. Chem. Rev.* **2015**, *293–294*, 263–278. [CrossRef]
2. Kang, X.-M.; Tang, M.-H.; Yang, G.-L.; Zhao, B. Cluster/cage-based coordination polymers with tetrazole derivatives. *Coord. Chem. Rev.* **2020**, *422*, 213424. [CrossRef]

3. Andruh, M. Oligonuclear complexes as tectons in crystal engineering: Structural diversity and magnetic properties. *Chem. Commun.* **2007**, 2565–2577. [CrossRef]

4. Roubeau, O.; Clérac, R. Rational assembly of high-spin polynuclear magnetic complexes into coordination networks: The case of a [Mn₄] single-molecule magnet building block. *Eur. J. Inorg. Chem.* **2008**, 4325–4342. [CrossRef]

5. Jeon, I.R.; Clerac, R. Controlled association of single-molecule magnets (SMMs) into coordination networks: Towards a new generation of magnetic materials. *Dalton Trans.* **2012**, *41*, 9569–9586. [CrossRef]

6. Shieh, M.; Liu, Y.-H.; Lia, Y.-H.; Lina, R.Y. Metal carbonyl cluster-based coordination polymers: Diverse syntheses, versatile network structures, and special properties. *Cryst. Eng. Comm.* **2019**, *21*, 7341–7364. [CrossRef]

7. Batten, S.R.; Neville, S.M.; Turner, D.R. *Coordination Polymers: Design, Analysis and Application*; Royal Society of Chemistry: Cambridge, UK, 2008; pp. 1–471.

8. Robson, R. A net-based approach to coordination polymers. *J. Chem. Soc. Dalton Trans.* **2000**, 3735–3744. [CrossRef]

9. Tranchemontagne, D.J.; Mendoza-Cortes, J.L.; O'Keeffe, M.; Yaghi, O.M. Secondary building units, nets and bonding in the chemistry of metal-organic frameworks. *Chem. Soc. Rev.* **2009**, 1257–1283. [CrossRef] [PubMed]

10. Eddaoudi, M.; Moler, D.B.; Li, H.; Chen, B.; Reineke, T.M.; O'Keeffe, M.; Yaghi, O.M. Modular chemistry: Secondary building units as a basis for the design of highly porous and robust metal-organic carboxylate frameworks. *Acc. Chem. Res.* **2001**, *34*, 319–330. [CrossRef]

11. Perry, J.J.; Permana, J.A.; Zaworotko, M.J. Design and synthesis of metal–organic frameworks using metal–organic polyhedra as supermolecular building blocks. *Chem. Soc. Rev.* **2009**, *38*, 1400–1417. [CrossRef] [PubMed]

12. Baca, S.G. The design of coordination networks from polynuclear Mn(II, III) and Fe(III) oxo-carboxylate clusters. In *Advances in Chemistry Research*; Taylor, J.C., Ed.; Nova Science Publishers: New York, NY, USA, 2018; Volume 43, pp. 81–130.

13. Fang, X.; Kögerler, P. A polyoxometalate-based manganese carboxylate cluster. *Chem. Commun.* **2008**, 3396–3398. [CrossRef] [PubMed]

14. Vaz, M.G.F.; Andruh, M. Molecule-based magnetic materials constructed from paramagnetic organic ligands and two different metal ions. *Coord. Chem. Rev.* **2021**, *427*, 213611. [CrossRef]

15. Ratera, I.; Veciana, J. Playing with organic radicals as building blocks for functional molecular materials. *Chem. Soc. Rev.* **2012**, *41*, 303–349. [CrossRef]

16. Kahn, O. Chemistry and physics of supramolecular magnetic materials. *Acc. Chem. Res.* **2000**, *33*, 647–657. [CrossRef] [PubMed]

17. Mccleverty, J.A.; Ward, M.D. The role of bridging ligands in controlling electronic and magnetic properties in polynuclear complexes. *Acc. Chem. Res.* **1998**, *31*, 842–851. [CrossRef]

18. Farrusseng, D. (Ed.) *Metal–Organic Frameworks. Applications from Catalysis to Gas Storage*; Wiley-VCH Verlag & Co. KgaA: Weinheim, Germany, 2011; p. 392.

19. Winpenny, R.E.P. (Ed.) *Single-Molecule Magnets and Related Phenomena*; Structure and Bonding; Springer: Berlin/Heidelberg, Germany, 2006; Volume 122.

20. Gatteschi, D.; Sessoli, R.; Villain, J. *Molecular Nanomagnets*; Oxford University Press: New York, NY, USA, 2006.

21. Gatteschi, D.; Sessoli, R.; Cornia, A. Single-molecule magnets based on iron(III) oxo clusters. *Chem. Commun.* **2000**, 725–732. [CrossRef]

22. Moushi, E.E.; Stamatatos, T.C.; Wernsdorfer, W.; Nastopoulos, V.; Christou, G.; Tasiopoulos, A.J. A Family of 3D coordination polymers composed of Mn₁₉ magnetic units. *Angew. Chem.* **2006**, *118*, 7886–7889. [CrossRef]

23. Moushi, E.E.; Stamatatos, T.C.; Wernsdorfer, W.; Nastopoulos, V.; Christou, G.; Tasiopoulos, A.J. A Mn₁₇ octahedron with a giant ground-state spin: Occurrence in discrete form and as multidimensional coordination polymers. *Inorg. Chem.* **2009**, *48*, 5049–5051. [CrossRef]

24. Moushi, E.E.; Stamatatos, T.C.; Wernsdorfer, W.; Nastopoulos, V.; Christou, G.; Tasiopoulos, A.J. 1-D coordination polymers consisting of a high-spin Mn₁₇ octahedral unit. *Polyhedron* **2009**, *28*, 1814–1817. [CrossRef]

25. Hessel, L.W.; Romers, C. The crystal structure of "anhydrous manganic acetate". *Recl. Trav. Chim. Pays-Bas* **1969**, *88*, 545–552. [CrossRef]

26. Albores, P.; Rentschler, E. Structural and magnetic characterization of a μ-1,5-dicyanamide-bridged iron basic carboxylate [Fe₃O(O₂C(CH₃)₃)₆] 1D chain. *Inorg. Chem.* **2008**, *47*, 7960–7962. [CrossRef]

27. Long, D.L.; Kögerler, P.; Farrugia, L.J.; Cronin, L. Linking chiral clusters with molybdate building blocks: From homochiral helical supramolecular arrays to coordination helices. *Chem. Asian J.* **2006**, *1*, 352–357. [CrossRef]

28. Wu, Q.L.; Han, S.D.; Wang, Q.L.; Zhao, J.P.; Ma, F.; Jiang, X.; Liu, F.C.; Bu, X.H. Divalent metal ions modulated strong frustrated M(II)–Fe(III)₃O (M = Fe, Mn, Mg) chains with metamagnetism only in a mixed valence iron complex. *Chem. Commun.* **2015**, *51*, 15336–15339. [CrossRef] [PubMed]

29. Baca, S.G.; Malaestean, I.L.; Keene, T.D.; Adams, H.; Ward, M.D.; Hauser, J.; Neels, A.; Decurtins, S. One-dimensional manganese coordination polymers composed of polynuclear cluster blocks and polypyridyl linkers: Structures and properties. *Inorg. Chem.* **2008**, *47*, 11108–11119. [CrossRef]

30. Dulcevscaia, G.M.; Filippova, I.G.; Speldrich, M.; Leusen, J.; Kravtsov, V.C.; Baca, S.G.; Kögerler, P.; Liu, S.X.; Decurtins, S. Cluster-based networks: 1D and 2D coordination polymers based on {MnFe₂(μ₃-O)}-type clusters. *Inorg. Chem.* **2012**, *51*, 5110–5117. [CrossRef] [PubMed]

31. Polunin, R.A.; Kiskin, M.A.; Cador, O.; Kolotilov, S.V. Coordination polymers based on trinuclear heterometallic pivalates and polypyridines: Synthesis, structure, sorption and magnetic properties. *Inorg. Chim. Acta* **2012**, *380*, 201–210. [CrossRef]

32. Lytvynenko, A.S.; Kiskin, M.A.; Dorofeeva, V.N.; Mishura, A.M.; Titov, V.E.; Kolotilov, S.V.; Eremenko, I.L.; Novotortsev, V.M. Redox-active porous coordination polymer based on trinuclear pivalate: Temperature-dependent crystal rearrangement and redox-behavior. *J. Solid State Chem.* **2015**, *223*, 122–130. [CrossRef]

33. Sotnik, S.A.; Polunin, R.A.; Kiskin, M.A.; Kirillov, A.M.; Dorofeeva, V.N.; Gavrilenko, K.S.; Eremenko, I.L.; Novotortsev, V.M.; Kolotilov, S.V. Heterometallic coordination polymers assembled from trigonal trinuclear Fe$_2$Ni-pivalate blocks and polypyridine spacers: Topological diversity, sorption, and catalytic properties. *Inorg. Chem.* **2015**, *54*, 5169–5181. [CrossRef] [PubMed]

34. Lytvynenko, A.S.; Polunin, R.A.; Kiskin, M.A.; Mishura, A.M.; Titov, V.E.; Kolotilov, S.V.; Novotortsev, V.M.; Eremenko, I.L. Electrochemical and electrocatalytic characteristics of coordination polymers based on trinuclear pivalates and heterocyclic bridging ligands. *Theor. Exp. Chem.* **2015**, *51*, 54–61. [CrossRef]

35. Zheng, Y.Z.; Tong, M.L.; Xue, W.; Zhang, W.X.; Chen, X.M.; Grandjean, F.; Long, G.J. A "Star" antiferromagnet: A polymeric iron(III) acetate that exhibits both spin frustration and long-range magnetic ordering. *Angew. Chem. Int. Ed.* **2007**, *46*, 6076–6080. [CrossRef]

36. Lytvynenko, A.S.; Kolotilov, S.V.; Cador, O.; Gavrilenko, K.S.; Golhen, S.; Ouahab, L.; Pavlishchuk, V.V. Porous 2D coordination polymeric formate built up by Mn(II) linking of Fe$_3$O units: Influence of guest molecules on magnetic properties. *Dalton Trans.* **2009**, 3503–3509. [CrossRef]

37. Polunin, R.A.; Kolotilov, S.V.; Kiskin, M.A.; Cador, O.; Mikhalyova, E.A.; Lytvynenko, A.S.; Golhen, S.; Ouahab, L.; Ovcharenko, V.I.; Eremenko, I.L.; et al. Topology control of porous coordination polymers by building block symmetry. *Eur. J. Inorg. Chem.* **2010**, 5055–5057. [CrossRef]

38. Dorofeeva, V.N.; Kolotilov, S.V.; Kiskin, M.A.; Polunin, R.A.; Dobrokhotova, Z.V.; Cador, O.; Golhen, S.; Ouahab, L.; Eremenko, I.; Novotortsev, V. 2D Porous honeycomb polymers versus discrete nanocubes from trigonal trinuclear complexes and ligands with variable topology. *Chem. Eur. J.* **2012**, *18*, 5006–5012. [CrossRef] [PubMed]

39. Botezat, O.; van Leusen, J.; Kravtsov, V.C.; Filippova, I.G.; Hauser, J.; Speldrich, M.; Hermann, R.P.; Krämer, K.W.; Liu, S.-X.; Decurtins, S.; et al. Interpenetrated (8,3)-c and (10,3)-b metal–organic frameworks based on {Fe$^{III}_3$} and {Fe$^{III}_2$Co^{II}} pivalate spin clusters. *Cryst. Growth. Des.* **2014**, *14*, 4721–4728. [CrossRef]

40. Zhao, J.P.; Han, S.D.; Jiang, X.; Xu, J.; Chang, Z.; Bu, X.H. A three dimensional magnetically frustrated metal–organic framework via the vertices augmentation of underlying net. *Chem. Commun.* **2015**, *51*, 4627–4630. [CrossRef] [PubMed]

41. Speldrich, M.; van Leusen, J.; Kögerler, P. CONDON 3.0: An updated software package for magnetochemical analysis - all the way to polynuclear actinide complexes. *J. Comput. Chem.* **2018**, *39*, 2133–2145. [CrossRef] [PubMed]

42. van Leusen, J.; Speldrich, M.; Schilder, H.; Kögerler, P. Comprehensive insight into molecular magnetism via CONDON: Full vs. Effective Models. *Coord. Chem. Rev.* **2015**, *289–290*, 137–148. [CrossRef]

43. Baca, S.G.; Filippova, I.G.; Keene, T.D.; Botezat, O.; Malaestean, I.L.; Stoeckli-Evans, H.; Kravtsov, V.C.; Chumacov, I.; Liu, S.-X.; Decurtins, S. Iron(III)-pivalate-based complexes with tetranuclear {Fe$_4$(μ_3-O)$_2$}$^{8+}$ cores and N-donor ligands: Formation of cluster and polymeric architectures. *Eur. J. Inorg. Chem.* **2011**, *3*, 356–367. [CrossRef]

44. Wang, S.; Tsai, H.L.; Folting, K.; Martin, J.M.; Hendrickson, D.N.; Christou, G. Covalent linkage of [Mn$_4$O$_2$(O$_2$CPh)$_6$(dbm)$_2$] into a dimer and a one-dimensional polymer (dbmH = dibenzoylmethane). *Chem. Commun.* **1994**, 671–673. [CrossRef]

45. Huang, D.; Zhang, X.; Ma, C.; Chen, H.; Chen, C.; Liu, Q.; Zhang, C.; Liao, D.; Li, L. Aggregation of tetranuclear Mn building blocks with alkali ion. Syntheses, crystal structures and chemical behaviors of monomer, dimer and polymer containing [Mn$_4$(μ_3-O)$_2$]$^{8+}$ units. *Dalton Trans.* **2007**, 680–688. [CrossRef]

46. Nakata, K.; Miyasaka, H.; Sugimoto, K.; Ishii, T.; Sugiura, K.; Yamashita, M. Construction of a one-dimensional chain composed of Mn$_6$ clusters and 4,4′-bipyridine linkers: The first step for creation of "Nano-Dots-Wires". *Chem. Lett.* **2002**, *31*, 658–659. [CrossRef]

47. Ma, C.-B.; Hu, M.Q.; Chen, H.; Chen, C.N.; Liu, Q.T. Aggregation of hexanuclear, mixed-valence manganese oxide clusters linked by propionato ligands to form a one-dimensional polymer [Mn$_6$O$_2$(O$_2$CEt)$_{10}$(H$_2$O)$_4$]$_n$. *Eur. J. Inorg. Chem.* **2008**, 5274–5280. [CrossRef]

48. Moushi, E.E.; Tasiopoulos, A.J.; Manos, M.J. Synthesis and structural characterization of a metal cluster and a coordination polymer based on the [Mn$_6$(μ_4-O)$_2$]$^{10+}$ unit. *Bioinorg. Chem. Appl.* **2010**, 367128. [CrossRef]

49. Malaestean, I.L.; Kravtsov, V.C.; Speldrich, M.; Dulcevscaia, G.; Simonov, Y.A.; Lipkowski, J.; Ellern, A.; Baca, S.G.; Kögerler, P. One-dimensional coordination polymers from hexanuclear manganese carboxylate clusters featuring a {Mn$^{II}_4$Mn$^{III}_2$(μ_4-O)$_2$} core and spacer linkers. *Inorg. Chem.* **2010**, *49*, 7764–7772. [CrossRef]

50. Darii, M.; Filippova, I.G.; Hauser, J.; Decurtins, S.; Liu, S.-X.; Kravtsov, V.C.; Baca, S.G. Incorporation of hexanuclear Mn(II,III) carboxylate clusters with a {Mn$_6$O$_2$} core in polymeric structures. *Crystals* **2018**, *8*, 100. [CrossRef]

51. Ovcharenko, V.; Fursova, E.; Romanenko, G.; Ikorskii, V. Synthesis and structure of heterospin compounds based on the [Mn$_6$(O)$_2$Piv$_{10}$]-cluster unit and nitroxide. *Inorg. Chem.* **2004**, *43*, 3332–3334. [CrossRef] [PubMed]

52. Baca, S.G.; Secker, T.; Mikosch, A.; Speldrich, M.; van Leusen, J.; Ellern, A.; Kögerler, P. Avoiding magnetochemical over-parametrization, exemplified by one-dimensional chains of hexanuclear iron(III) pivalate clusters. *Inorg. Chem.* **2013**, *52*, 4154–4156. [CrossRef] [PubMed]

53. Fursova, E.Y.; Ovcharenko, V.I.; Bogomyakov, A.S.; Romanenko, G.V. Structure of the complex of hexanuclear manganese pivalate with isonicotinamide. *J. Struct. Chem.* **2013**, *54*, 164–167. [CrossRef]

54. Malaestean, I.L.; Ellern, A.; van Leusen, J.; Kravtsov, V.C.; Kögerler, P.; Baca, S.G. Cluster-based networks: Assembly of a (4,4) layer and a rare T-shaped bilayer from $[Mn^{III}_2Mn^{II}_4O_2(RCOO)_{10}]$ coordination clusters. *Cryst. Eng. Comm.* **2014**, *16*, 6523–6525. [CrossRef]

55. Kar, P.; Haldar, R.; Gómez-García, C.J.; Ghosh, A. Antiferromagnetic porous metal–organic framework containing mixed-valence $[Mn^{II}_4Mn^{III}_2(\mu_4\text{-O})_2]^{10+}$ units with catecholase activity and selective gas adsorption. *Inorg. Chem.* **2012**, *51*, 4265–4273. [CrossRef]